Cooperative spontaneous emission of three identical atoms

Wei Feng, Yong Li, and Shi-Yao Zhu
Beijing Computational Science Research Center, Beijing 100084, China
(Received 5 February 2013; published 30 September 2013)

We study cooperative single-photon spontaneous emission from three multilevel atoms with one of them being excited for different atomic configurations in optical vector theory. The dynamic evolution is solved by finding the eigenvalues of a 3×3 matrix, and then the relevant decay rates and Lamb shifts are obtained analytically. It is shown that the symmetry of atomic configuration has a big influence on the super-radiance of the system. To obtain strong super-radiance requires not only the distances among the three atoms to be much shorter than the wavelength, but also to have symmetrical distribution. We also calculate the emission spectra and find that it normally has three peaks, but it has two peaks under the equilateral-triangle configuration.

DOI: 10.1103/PhysRevA.88.033856 PACS number(s): 42.50.Nn, 42.50.Ct, 03.65.Yz

I. INTRODUCTION

The spontaneous emission spectra and Lamb shift of an independent atom once stimulated the development of quantum theory and quantum electrodynamics. The cooperative spontaneous emission was first investigated by Dicke in 1954 [1], where the dimension of atomic ensemble is smaller than the involved emission wavelength, and he found that the strong coupling between atoms can greatly enhance or suppress the spontaneous emission, called the super- and subradiance, respectively. After the pioneering work by Dicke, the phenomena of super- and subradiance were extensively studied by different methods with different models [2–7]. In the study of decay dynamics, the rotating-wave approximation (RWA) is a good approximation as the counter-rotating terms formally violate the energy conservation, and only lead to virtual processes. However, the virtual processes really exist and are the origin of Lamb shift. The counter-rotating terms must be considered if we want to calculate the collective Lamb shift of coherent atomic systems. Recently, the collective spontaneous emission and Lamb shift from the N-atom system including the counter-rotating terms and virtual photons were extensively discussed by Scully's group [8–12] and others [13–15]. They found that the virtual processes (the counter-rotating terms) could have a significant effect on the time evolution of the system. Meanwhile, the experimental research about collective Lamb shift also made progress [16,17]. In the above theoretical research [8–15], the authors adopted several assumptions to simplify the calculation. One of the assumptions is the scalar photon theory in which the polarization and vector character of the field is ignored.

In our previous works [18,19], we studied a similar system by optical vector theory where all possible wave-vector directions and polarizations of the vacuum modes in the three-dimensional space are taken into account. Meanwhile, a unitary transformation method we previously developed [20–22] could effectively help us to solve the effects of the counter-rotating terms. Finally, by numerical calculation, we studied the influence of ensemble volume, density, and the effect of geometry on cooperative spontaneous emission. In short, the model in Refs. [18,19] is similar to that in the previous papers [8–15], where a large number of atoms are randomly distributed in a fixed volume. Due to the large number of atoms, it is impossible to derive an analytic solution, and numerical computation is usually required. In another paper [23], a system of two identical atoms is studied, where the analytic expression for the decay rate and Lamb shift was obtained, and their dependence on the distance between the two atoms was studied.

In this paper, we consider the system of three multilevel atoms with optical vector theory. The problem of dynamic evolution is transformed to an eigenvalue problem of a 3×3 matrix. Especially, we can get an analytic solution beyond the numerical calculation and use it to analyze the influence of atomic configuration on the decay rates and Lamb shifts. We find that the atomic configuration has a great impact on the dynamical evolution and emission spectra of the system. The results of this paper may be valuable to experimental research of coupled quantum dots where the configuration can be easily controlled, and the cooperative spontaneous emission of quantum dots is a new focus of research [24–27].

This paper is prepared as follows: In Sec. II, we give the model and Hamiltonian of system, and apply the unitary transformation to the Hamiltonian. In Sec. III, we derive the analytic expression of three eigenvalues associated with three exponentially decaying eigenstates under the Weisskopf-Wigner approach. In Sec. IV, we apply the analytic solution to several different atomic configurations, and calculate the decay rates and Lamb shift, respectively. In Sec. V, the expression of the spontaneous emission spectrum is given and the spectra under several different conditions are plotted. At last, a summary is given in Sec. VI.

II. MODEL AND HAMILTONIAN

We consider the system consists of three identical multilevel atoms interacting with the vacuum field. The atoms are fixed in space and labeled 1, 2, and 3, respectively. The Hamiltonian of the system can be written as ($\hbar = 1$) [6], [23]

$$H = H_0 + H_I + H_{d-d}, \tag{1}$$

where H_0 is the unperturbed Hamiltonian of the atoms and vacuum field, H_I is the interaction Hamiltonian between the atoms and the vacuum modes, and H_{d-d} is the electrostatic dipole-dipole interaction Hamiltonian between

the atoms,

$$H_0 = \sum_n \sum_i \omega_i |i\rangle_n \langle i|_n + \sum_{\mathbf{k}} \omega_k b_{\mathbf{k}}^\dagger b_{\mathbf{k}}, \tag{2}$$

$$H_I = \sum_{n,\mathbf{k}} \sum_{j\neq i} g_{\mathbf{k},ij} |i\rangle_n \langle j|_n (b_{\mathbf{k}}^\dagger e^{-i\mathbf{k}\cdot\mathbf{r_n}} + b_{\mathbf{k}} e^{i\mathbf{k}\cdot\mathbf{r_n}}), \tag{3}$$

$$H_{d-d} = \frac{1}{4\pi\varepsilon_0} \sum_{m<n} \left[\frac{\mathbf{d}^{(m)}\cdot\mathbf{d}^{(n)}}{r_{mn}^3} - \frac{3(\mathbf{d}^{(m)}\cdot\mathbf{r}_{mn})(\mathbf{d}^{(n)}\cdot\mathbf{r}_{mn})}{r_{mn}^5} \right], \quad m,n = 1,2,3. \tag{4}$$

Here ω_i is the energy of level $|i\rangle$, $b_{\mathbf{k}}^\dagger$ ($b_{\mathbf{k}}$) is the creation (annihilation) operator of the $\mathbf{k}$th mode with frequency ω_k, and $g_{\mathbf{k},ij} = \omega_{ij} d_{ij} (2\varepsilon_0 \omega_k V)^{-1/2} \hat{e}_{\mathbf{k}} \hat{\mathbf{d}}_{ij}$ is the coupling strength between the $\mathbf{k}$th electromagnetic mode with unit polarization vector $\hat{e}_{\mathbf{k}}$ and the atomic transition between levels $|i\rangle$ and $|j\rangle$ with transition dipole moment $\mathbf{d}_{ij} = \mathrm{e}\langle i|\mathbf{r}|j\rangle = d_{ij}\hat{\mathbf{d}}_{ij}$, of which d_{ij} (assumed to be real) and $\hat{\mathbf{d}}_{ij}$ are the magnitude and unit vector, respectively. The nth atom is located at position $\mathbf{r}_n$ and the displacement between the mth and nth atoms is $\mathbf{r}_{mn} \equiv \mathbf{r}_n - \mathbf{r}_m \equiv r_{mn}\hat{\mathbf{r}}_{mn}$. In Eq. (4), $\mathbf{d}^{(n)} = \sum_{ij} \mathbf{d}_{ij} |i\rangle_n \langle j|_n$ is the operator of the dipole moment for the nth atom. We assume that the three atoms have the same direction of dipole moment which can be realized in experiment. The angle between the dipole moment and the vector $\mathbf{r}_{mn}$ is η_{mn}, as shown in Fig. 1.

In order to take into account the counter-rotating terms and simplify the calculation, we introduce a unitary transformation $U = \exp(iS)$ with [20]

$$S = \sum_{n,\mathbf{k}} \sum_{j\neq i} \frac{g_{\mathbf{k},ij}\xi_{k,ij}}{i\omega_k} |i\rangle_n \langle j|_n (b_{\mathbf{k}}^\dagger e^{-i\mathbf{k}\cdot\mathbf{r}_n} - b_{\mathbf{k}} e^{i\mathbf{k}\cdot\mathbf{r}_n}), \tag{5}$$

where $\xi_{k,ij} = \omega_k/(\omega_k + |\omega_{ji}|)$ and $\omega_{ji} \equiv \omega_j - \omega_i$. By subtracting the free-electron self-energy $E_{se} = -\sum_{n,j\neq i} \sum_{\mathbf{k}} (|g_{\mathbf{k},ij}|^2/\omega_k) |i\rangle_n \langle i|_n$, the effective Hamiltonian after the transformation can be written as

$$\begin{aligned} H^S &= e^{iS} H e^{-iS} - E_{se} \\ &= H_0 + (H_0' - E_{se}) + H_I' + H_{i\mathrm{v}} + H_{d-d} + o\left(g_{\mathbf{k},ij}^2\right), \end{aligned} \tag{6}$$

where

$$H_0' - E_{se} = \sum_{n,\mathbf{k}} \sum_{j\neq i} \frac{|g_{\mathbf{k},ij}|^2}{\omega_k} \left(\xi_{k,ij}^2 + \frac{\omega_{ji}}{\omega_k} \xi_{k,ij}^2 - 2\xi_{k,ij} + 1 \right) \times |i\rangle_n \langle i|_n, \tag{7}$$

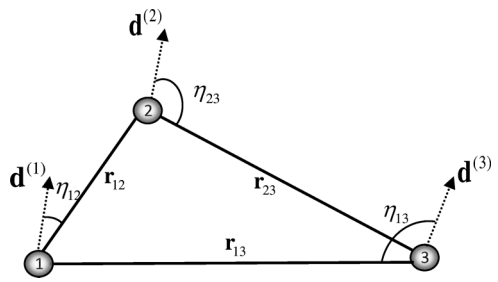

FIG. 1. The schematic description of the relation between dipoles and displacements.

$$H_I' = \sum_{n,\mathbf{k}} \sum_{i<j} V_{\mathbf{k},ij} (|i\rangle_n \langle j|_n b_{\mathbf{k}}^\dagger e^{-i\mathbf{k}\cdot\mathbf{r_n}} + |j\rangle_n \langle i|_n b_{\mathbf{k}} e^{i\mathbf{k}\cdot\mathbf{r_n}}), \tag{8}$$

$$H_{i\mathrm{v}} = -\sum_{m<n,\mathbf{k}} \sum_{i,i',j,j'} \frac{2g_{\mathbf{k},ij} g_{\mathbf{k},i'j'} \xi_{k,ij}}{\omega_k} (2 - \xi_{k,i'j'}) |i\rangle_m \times \langle j|_m \otimes |i'\rangle_n \langle j'|_n e^{i\mathbf{k}\cdot\mathbf{r}_{mn}}. \tag{9}$$

Here $H_0' - E_{se}$ only contains the diagonal energy corrections, which is called the nondynamic shift for single atoms. H_I' is the transformed interaction Hamiltonian between the atoms and the vacuum modes, and $V_{\mathbf{k},ij} = g_{\mathbf{k},ij}\, 2|\omega_{ji}|/(\omega_k + |\omega_{ji}|)$ is the transformed coupling strength. $H_{i\mathrm{v}}$ is the interaction Hamiltonian due to exchange of virtual photons. Note that after the unitary transformation, H_I' has a RWA-like form and H_{d-d} does not change its form because it commutes with S.

III. DYNAMIC EVOLUTION

Here we consider the initial state that on average has one atom in the first excited state and the other two in the ground state, which can be called the single-photon state [8–19]. We denote the ground and first excited levels of the identical atoms as $|g\rangle$ and $|e\rangle$, respectively. In the transformed total Hamiltonian H^S, the zeroth term $H_0^S := H_0 + (H_0' - E_{se})$ can be rewritten as

$$H_0^S = \sum_{\mathrm{n}} \sum_i \omega_i' |i\rangle_n \langle i|_n + \sum_{\mathbf{k}} \omega_k b_{\mathbf{k}}^\dagger b_{\mathbf{k}}, \tag{10}$$

where we have introduced the effective state energies $\omega_i' = \omega_i + \delta_i^{nd}$ with the nondynamic shift for single atoms,

$$\delta_i^{nd} = \sum_{j\neq i,\mathbf{k}} \frac{|g_{\mathbf{k},ij}|^2}{\omega_k} \left(\xi_{k,ij}^2 + \frac{\omega_{ji}}{\omega_k} \xi_{k,ij}^2 - 2\xi_{k,ij} + 1 \right). \tag{11}$$

In the interaction picture with respect to H_0^S, the interaction Hamiltonian becomes

$$H_{IP} = e^{iH_0^S t} (H_I' + H_{i\mathrm{v}} + H_{d-d}) e^{-iH_0^S t} = H_I^{IP} + H_{sta}^{IP}, \tag{12}$$

where

$$H_I^{IP} = \sum_{n,\mathbf{k}} V_{\mathbf{k},eg} (|g\rangle_n \langle e|_n b_{\mathbf{k}}^\dagger e^{-i(\omega_{eg}' - \omega_k)t} e^{-i\mathbf{k}\cdot\mathbf{r_n}} + |e\rangle_n \langle g|_n b_{\mathbf{k}} e^{i(\omega_{eg}' - \omega_k)t} e^{i\mathbf{k}\cdot\mathbf{r_n}}), \tag{13}$$

$$\begin{aligned} H_{sta}^{IP} &= H_{i\mathrm{v}}^{IP} + H_{d-d}^{IP} = H_{i\mathrm{v}} + H_{d-d} \\ &= \sum_{m<n} \Delta_{\mathrm{sta}}^{mn} (|e_m\rangle \langle e_n| + |e_n\rangle \langle e_m|), \end{aligned} \tag{14}$$

$$\Delta_{sta}^{mn} = \frac{1}{4\pi\varepsilon_0} \left[\frac{\mathbf{d}_{eg}^{(m)}\cdot\mathbf{d}_{ge}^{(n)}}{r_{mn}^3} - \frac{3\left(\mathbf{d}_{eg}^{(m)}\cdot\mathbf{r}_{mn}\right)\left(\mathbf{d}_{ge}^{(n)}\cdot\mathbf{r}_{mn}\right)}{r_{mn}^5} \right] - \sum_{\mathbf{k}} \frac{2g_{\mathbf{k},eg}^2 \xi_{k,eg}}{\omega_k} (2 - \xi_{k,eg}) e^{i\mathbf{k}\cdot\mathbf{r_{mn}}}. \tag{15}$$

Here the quasistatic shift Δ_{sta}^{mn} comes from the electrostatic dipole-dipole interaction and the interaction due to exchange

of virtual photons. The state $|e_n\rangle$ stands for the one where the nth atom is in the first excited level and the others are in their ground levels. In the interaction picture, the wave function at time t can be written as

$$|\psi(t)\rangle = \sum_n C_n(t)\,|e_n;0\rangle + \sum_{\mathbf{k}} C_{\mathbf{k}}(t)\,|G;1_{\mathbf{k}}\rangle, \tag{16}$$

where the state $|G;1_{\mathbf{k}}\rangle$ represents the three atoms all in the ground state and a single photon in mode $\mathbf{k}$, and $|e_n;0\rangle$ stands for the state where only the nth atom is in its excited level and the electromagnetic field is in the vacuum state. From the Schrödinger equation $i\partial_t|\psi(t)\rangle = H_{IP}|\psi(t)\rangle$, we obtain the equations of motion for the state amplitudes,

$$\dot{C}_n(t) = -i\sum_{\mathbf{k}} V_{\mathbf{k},eg} e^{i(\omega'_{eg}-\omega_k)t} e^{i\mathbf{k}\cdot\mathbf{r_n}} C_{\mathbf{k}}(t) - i\sum_{m\neq n}\Delta^{mn}_{sta} C_m(t), \tag{17}$$

$$\dot{C}_{\mathbf{k}}(t) = -i\sum_n V_{\mathbf{k},eg} e^{-i(\omega'_{eg}-\omega_k)t} e^{-i\mathbf{k}\cdot\mathbf{r_n}} C_n(t). \tag{18}$$

Formally integrating Eq. (18) with the initial value $C_{\mathbf{k}}(0)=0$, and extending the lower bound of time integration to $-\infty$ under the Weisskopf-Wigner approximation at the long time limit, we get

$$C_{\mathbf{k}}(t) = -i\sum_n V_{\mathbf{k},eg} e^{-i\mathbf{k}\cdot\mathbf{r_n}} \int_{-\infty}^{t} e^{-i(\omega'_{eg}-\omega_k)t'} C_n(t')dt'. \tag{19}$$

Substituting Eq. (19) into Eq. (17), and replacing $C_n(t')$ in the time integration by $C_n(t)$ under the Markov approximation, we find

$$\begin{aligned}\dot{C}_n(t) \approx& -C_n(t)\sum_{\mathbf{k}} V^2_{\mathbf{k},eg}\int_{-\infty}^{t} e^{i(\omega'_{eg}-\omega_k)(t-t')}dt' \\ &- C_m(t)\sum_{m\neq n}\left[\sum_{\mathbf{k}} V^2_{\mathbf{k},eg} e^{ikr_{nm}}\int_{-\infty}^{t} e^{i(\omega'_{eg}-\omega_k)(t-t')}dt' \right. \\ &\left. + i\,\Delta^{mn}_{sta}\right] \\ =& -\Gamma_0 C_n(t) - \sum_{m\neq n}\Gamma_{mn} C_m(t),\end{aligned} \tag{20}$$

where

$$\Gamma_0 = \frac{\gamma_{eg}}{2} + i\,\Delta_{eg}, \tag{21}$$

$$\Gamma_{mn} = \frac{\gamma_{eg}}{2}\left[D(x_{mn},\eta_{mn}) + i\,P(x_{mn},\eta_{mn})\right]. \tag{22}$$

The detailed derivation of the above equations is shown in the Appendix. In the above formulas, $\gamma_{eg}=\frac{d^2_{eg}\omega^3_{eg}}{3\pi\varepsilon_0 c^3}$ is the standard single-atom decay rate from $|e\rangle$ to $|g\rangle$, Δ_{eg} is the dynamic shift of single atoms, and $x_{mn} := \frac{r_{mn}}{\lambda_0}$ (λ_0 is the wavelength of the resonantly emitted photon). $D(x,\eta)$ and $P(x,\eta)$ are two dimensionless functions,

$$\begin{aligned}D(x,\eta) =& \frac{3}{2}\left\{\sin^2\eta\,\frac{\sin(2\pi x)}{2\pi x}\right. \\ &\left. + (1-3\cos^2\eta)\left[\frac{\cos(2\pi x)}{(2\pi x)^2} - \frac{\sin(2\pi x)}{(2\pi x)^3}\right]\right\},\end{aligned} \tag{23}$$

$$\begin{aligned}P(x,\eta) =& \frac{3}{2}\left\{-\sin^2\eta\,\frac{\cos(2\pi x)}{2\pi x}\right. \\ &\left. + (1-3\cos^2\eta)\left[\frac{\sin(2\pi x)}{(2\pi x)^2} + \frac{\cos(2\pi x)}{(2\pi x)^3}\right]\right\}.\end{aligned} \tag{24}$$

From Eq. (22) we can see the two dimensionless functions $D(x,\eta)$ and $P(x,\eta)$ describe the influence of interaction between atoms on the decay rate and Lamb shift, respectively. In Fig. 2, we plot the two dimensionless functions versus x for different angle η, where we can see both functions show oscillatory characteristics and a strong dependence on the direction of dipole moment. Especially when $x\to 0$, $P(x,\eta)$ is divergent as x^{-3} and it can be either positive or negative for different η. Note that $D(x,\eta)$ and $P(x,\eta)$ oscillate with the largest amplitude when $\eta=\frac{\pi}{2}$, since the radiation is strongest in the direction perpendicular to the dipole.

The coefficients in the differential equation (20) constitute a symmetric 3×3 matrix

$$\mathbf{\Gamma} = \begin{bmatrix}\Gamma_0 & \Gamma_{12} & \Gamma_{13}\\ \Gamma_{12} & \Gamma_0 & \Gamma_{23}\\ \Gamma_{13} & \Gamma_{23} & \Gamma_0\end{bmatrix}. \tag{25}$$

Now the problem is to find the complex eigenvalues Γ_m and eigenvectors $|\Gamma_m\rangle$ of the matrix $\mathbf{\Gamma}$. The eigenvalue problem of an $n\times n$ matrix is to solve an nth degree algebraic equation, and it is well known that there is no radical solution of high-degree equation (above quartic equation). Here, by solving a cubic equation, we can obtain the analytic expressions of three eigenvalues as

$$\begin{aligned}\Gamma_a &= \Gamma_0 + \frac{\sqrt{3}}{3}\sqrt{\Gamma^2_{12}+\Gamma^2_{13}+\Gamma^2_{23}}\left(\cos\frac{\theta}{3} + \sqrt{3}\sin\frac{\theta}{3}\right)\\ \Gamma_b &= \Gamma_0 + \frac{\sqrt{3}}{3}\sqrt{\Gamma^2_{12}+\Gamma^2_{13}+\Gamma^2_{23}}\left(\cos\frac{\theta}{3} - \sqrt{3}\sin\frac{\theta}{3}\right),\\ \Gamma_c &= \Gamma_0 - \frac{2\sqrt{3}}{3}\sqrt{\Gamma^2_{12}+\Gamma^2_{13}+\Gamma^2_{23}}\cos\frac{\theta}{3}\end{aligned} \tag{26}$$

where $\theta = \arccos T$ with $T = -3\sqrt{3}\Gamma_{12}\Gamma_{13}\Gamma_{23}(\Gamma^2_{12}+\Gamma^2_{13}+\Gamma^2_{23})^{-(3/2)}$. The expression of the eigenvectors can be obtained, but the calculation is tedious. Basing on the results of these eigenvalues and eigenvectors, we can know the dynamic evolution of the system. For any initial state $|\psi(0)\rangle = \sum_{m=1}^{3} a_m|\Gamma_m\rangle$, the wave function at time t is

$$|\psi(t)\rangle = \sum_m a_m e^{-\Gamma_m t}\,|\Gamma_m\rangle. \tag{27}$$

IV. DECAY RATES AND LAMB SHIFT

The three complex eigenvalues in Eq. (26) can be written as the form

$$\Gamma_{a,b,c} = \frac{\gamma_{a,b,c}}{2} + i\,\delta_{a,b,c}, \tag{28}$$

where $\gamma_{a,b,c}$ and $\delta_{a,b,c}$ are the decay rates and the Lamb shifts of the three eigenstates in a long time limit. With Eq. (26) we can calculate the decay rates and Lamb shifts for any atomic

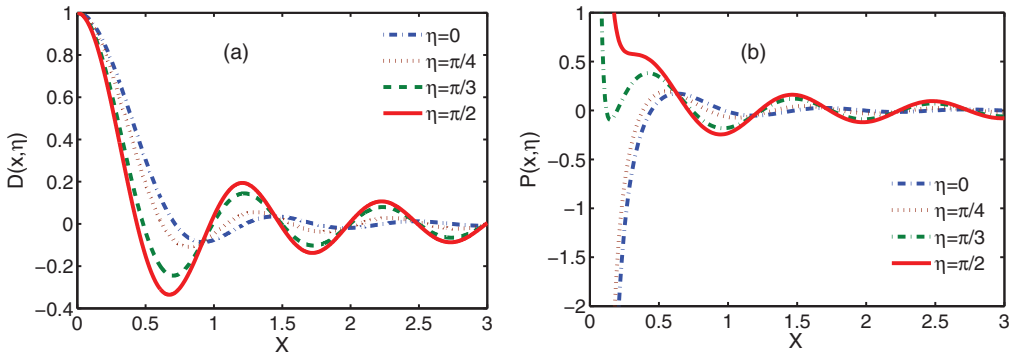

FIG. 2. (Color online) (a) $D(x,\eta)$ and (b) $P(x,\eta)$ versus x with different η.

configuration of the system. Now we consider three different cases.

A. Equilateral triangle

Firstly, we consider the most symmetric case: The three atoms are arranged as an equilateral triangle ($r_{mn} = r$) and the dipole moment is perpendicular to the plane of the three atoms ($\eta_{mn} = \eta = \pi/2$). In this case, the three atoms are equivalent and all the off-diagonal elements Γ_{mn} are the same (denoted as Γ_1). Then Eq. (26) can be simplified as

$$\Gamma_a = \Gamma_0 + 2\Gamma_1, \quad \Gamma_b = \Gamma_c = \Gamma_0 - \Gamma_1. \tag{29}$$

Note that Γ_b and Γ_c are the same, so the corresponding eigenstates $|b\rangle$ and $|c\rangle$ are not unique. The three exponentially decaying eigenstates can be written as

$$\begin{aligned} |a\rangle &= \frac{1}{\sqrt{3}}\left(|e_1\rangle + |e_2\rangle + |e_3\rangle\right), \\ |b\rangle &= \frac{1}{\sqrt{2}}\left(|e_2\rangle - |e_3\rangle\right), \\ |c\rangle &= \frac{1}{\sqrt{6}}\left(|e_2\rangle + |e_3\rangle - 2\,|e_1\rangle\right). \end{aligned} \tag{30}$$

Notice that the eigenstate $|a\rangle$ is the Dicke state, $|D\rangle = \frac{1}{\sqrt{N}}\sum_n |e_n\rangle$ [8], of the three-atom system, where each atom has the same probability in its excited level with the same phase. From the matrix $\mathbf{\Gamma}$, we can see that the Dicke state is an eigenstate of the system only when all the off-diagonal elements Γ_{mn} are the same, and this condition can be satisfied only in the special equilateral-triangle case for a three-atom system. Previously, it was proven that the Dicke state is an eigenstate in a two-atom system [23]. Here, we can obtain the further conclusion that the Dicke state cannot exactly be an exponentially decaying eigenstate in an $N-$atom system if $N \geqslant 4$, because there is no atomic space distribution resulting in the same interactions between any two atoms. For example, in the system of $N = 4$, the four atoms can be distributed as a regular tetrahedron, where the distances between any two atoms are equal, but the same angle η_{mn} cannot be achieved, so that the off-diagonal elements will not be equal, and the Dicke state will not be an eigenstate for the system.

According to Eqs. (28) and (29), we can obtain the decay rates of three eigenstates,

$$\begin{aligned} \gamma_a &= \gamma_{\rm eg}\left[1 + 2D\left(x, \frac{\pi}{2}\right)\right], \\ \gamma_b &= \gamma_c = \gamma_{\rm eg}\left[1 - D\left(x, \frac{\pi}{2}\right)\right], \end{aligned} \tag{31}$$

where $x \equiv r/\lambda_0$. The modifications of the decay rates are completely determined by $D(x, \frac{\pi}{2})$. From Fig. 2(a), we know that when the atomic distance is smaller than the resonant wavelength, the value of the function $D(x, \frac{\pi}{2})$ is large, and the interaction between atoms can greatly change the collective decay rates of the system. Especially with the atomic distance tending to zero, $D(x, \frac{\pi}{2})$ approaches its maximum value 1, and consequently, the decay rate of the Dicke state $|a\rangle$ will increase to triple the decay rate of a single atom (the limit of three-atom super-radiance), while the decay rates of $|b\rangle$ and $|c\rangle$ tend to zero. Note that $D(x, \frac{\pi}{2})$ can be negative at some ranges of distance [see Fig. 2(a)], so that the Dicke state is not super-radiant under this condition. This phenomenon can be explained as follows. If the distance is around the odd times of the half wavelength [the negative part of $D(x,\eta)$ in Fig. 2(a)], the emissions from different atoms are out of phase and the destructive interference will suppress the collective spontaneous emission; thus the Dicke state is subradiant under this condition.

Next, we discuss the Lamb shift of three eigenstates. Similar to Eq. (31), we can obtain

$$\begin{aligned} \delta_a &= \Delta_{eg} + \gamma_{eg} P\left(x, \frac{\pi}{2}\right), \\ \delta_b &= \delta_c = \Delta_{eg} - \frac{\gamma_{eg}}{2} P\left(x, \frac{\pi}{2}\right). \end{aligned} \tag{32}$$

As mentioned above, Δ_{eg} is the dynamic shift of single atoms, and its concrete form is shown in the Appendix. Here we mainly focus on the shifts that come from the interaction between atoms (the collective Lamb shift), represented by the second terms in Eq. (32). Note that the Lamb shifts of $|b\rangle$ and $|c\rangle$ are the same, i.e., the two states are degenerated due to the symmetry. The energy differences between the Dicke state and the other two states are

$$\delta_a - \delta_b = \delta_a - \delta_c = \frac{3}{2}\gamma_{eg} P\left(x, \frac{\pi}{2}\right). \tag{33}$$

This tells us that the splitting between the states is determined by $P(x, \frac{\pi}{2})$, which describes the dipole-dipole interaction

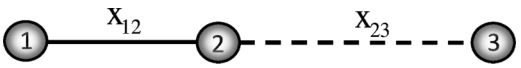

FIG. 3. The schematic description of the atomic configuration of a straight line.

arising from the real and virtual photon exchange between the atoms. This kind of interaction results in the collective Lamb shift which is significantly dependent on the distances between the atoms and will change its sign with the distance increasing; see Fig. 2(b).

B. Straight line

Now we consider the configuration where three atoms are arranged in a straight line, as shown in Fig. 3. Here we fix $\eta_{mn} = \pi/2$. According to Eqs. (26) and (28), we plot the decay rates of the three eigenstates $\gamma_{a,b,c}$ as a function of x_{23} with different x_{12} in Fig. 4.

From Figs. 4(a)–4(d), we can see that the decay rate of the super-radiant state reaches its maximum at different x_{23}. For large x_{12} (comparable to or larger than the wavelength), the maximum decay rate is at $x_{23} = 0$ [see the blue solid line in Fig. 4(a)], because the dipole-dipole interaction between the first and second (and third) atoms is weak and the three-atom system reduces to the two-atom system consisting of the second and third atoms where the strongest super-radiance happens at $x_{23} \to 0$, plus the single first atom (weak coupled). With x_{12} decreasing, the distance x_{23} at which we have the maximum decay rate approaches $x_{23} = x_{12}$ [see the blue solid line in Figs. 4(c) and 4(d)]. That is to say, the super-radiance also depends on the details of atom configuration (distribution).

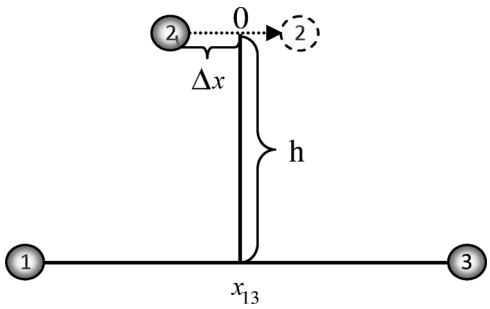

FIG. 5. The schematic description of the atomic configuration of a general triangle. Here $x_{13} = 0.1$, $h = 0.05$, and Δx is the displacement related to the central vertical line. All the distances are in units of λ_0.

In order to approach the limit of Dicke super-radiance $3\gamma_{eg}$, we not only need the short enough total length x_{13}, but we also need the symmetry distribution $x_{23} = x_{12}$.

C. General triangle: The effect of symmetry

Next, we investigate the influence of symmetrical distribution on the super-radiance of the system by considering the general-triangle configuration where the first and third atoms are fixed as the base and the second atom stays at a different position around the central vertical line, as shown in Fig. 5.

We select a short distance between the first and third atom and a short height of the triangle, $x_{13} = 0.1$, $h = 0.05$, respectively, which guarantees the strong dipole-dipole interaction among the three atoms. With this configuration and $\eta_{mn} = \pi/2$, we discuss the influence of symmetry on

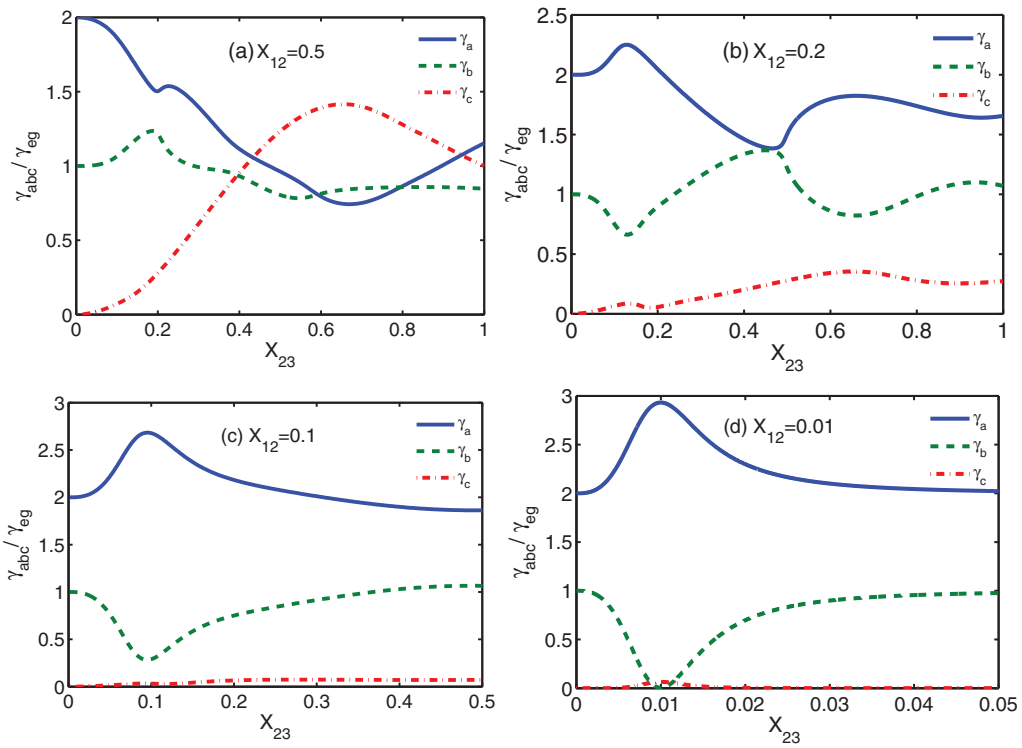

FIG. 4. (Color online) The decay rates of the three eigenstates as a function of x_{23} with (a) $x_{12} = 0.5$, (b) $x_{12} = 0.2$, (c) $x_{12} = 0.1$, and (d) $x_{12} = 0.01$. Here $\eta_{mn} = \pi/2$ and all the distances are in units of λ_0.

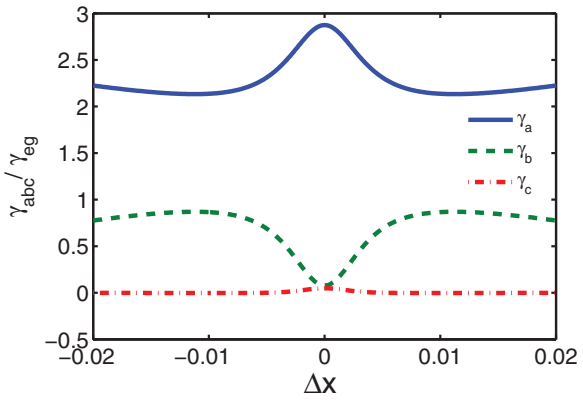

FIG. 6. (Color online) The decay rates of three eigenstates as a function of Δx. Here $\eta_{mn} = \pi/2$.

the super-radiance by changing Δx. In Fig. 6, we plot three eigendecay rates as a function of displacement Δx. It is clear that the maximal decay rate of super-radiance is obtained at symmetrical distribution $\Delta x = 0$ ($x_{23} = x_{12}$). Actually, from the perspective of the matrix [Eq. (25)], the general-triangle configuration is similar to the straight-line configuration where the three off-diagonal elements have different values, but when $x_{23} = x_{12}$, two of them are equal.

To explain the symmetric effect that occurred in the straight-line and general-triangle configurations, we go back to the matrix in Eq. (25). When $x_{23} = x_{12}$, the corresponding off-diagonal elements have $\Gamma_{12} = \Gamma_{23}$. The analytic expressions of three eigenvalues in Eq. (26) can be simplified as

$$\begin{aligned}\Gamma_a &= \Gamma_0 + \frac{\Gamma_{13}+\sqrt{\Gamma_{13}^2+8\Gamma_{12}^2}}{2},\\ \Gamma_b &= \Gamma_0 - \Gamma_{13},\\ \Gamma_c &= \Gamma_0 + \frac{\Gamma_{13}-\sqrt{\Gamma_{13}^2+8\Gamma_{12}^2}}{2}.\end{aligned} \tag{34}$$

When the distances between the three atoms are all smaller enough than the wavelength, the real parts of the three off-diagonal elements are approximately equal to 1, see Fig. 2(a), while the imaginary parts, the function $P(x,\eta)$, is divergent when $x \to 0$, so we can make the assumption that $P(x_{12},\eta_{12}) \gg P(x_{13},\eta_{13}) \gg 1$ and $D(x_{12},\eta_{12}) = D(x_{13},\eta_{13}) = 1$. Consequently, we can estimate that $\sqrt{\Gamma_{13}^2+8\Gamma_{12}^2} \approx 2\sqrt{2}\Gamma_{12}$, and according to Eq. (28), we have

$$\begin{aligned}\gamma_a &\approx \gamma_{eg}\left(1+\frac{1+2\sqrt{2}}{2}\right) \approx 2.91\gamma_{eg},\\ \gamma_b &\approx 0,\\ \gamma_c &\approx \gamma_{eg}\left(1+\frac{1-2\sqrt{2}}{2}\right) \approx 0.09\gamma_{eg}.\end{aligned} \tag{35}$$

Note that the approximate results of super-radiant decay rate $2.91\gamma_{eg}$ are close to the limit of $3\gamma_{eg}$ and coincident with the maximum decay rate of super-radiance in Fig. 6.

From the above analysis, we can see that the symmetric effect is universal for a strong coupling three-atom system. The physical interpretation is that when the three atoms are distributed symmetrically, the photons can be uniformly exchanged among them and as a whole they can display the strong super-radiance. The symmetric effect of the distribution in the three-atom system can extend to a multiatom system: The uniform distribution of atoms is beneficial to realizing the strong super-radiance of the system. The physical interpretation is the same as that in the three-atom system. Note that in the above latter two atomic configurations, we do not discuss the Lamb shift and the influence of direction of dipole moment. Next, we study these by the emission spectra.

V. SPECTRUM

The probability of the detector absorbing a photon from the field at position $\mathbf{R}$ and time t is proportional to the Glauber's first-order correlation function [28],

$$\begin{aligned}G_1(\mathbf{R},t) &= \langle\psi_F|\, E^{(-)}(\mathbf{R},t)E^{(+)}(\mathbf{R},t)\,|\psi_F\rangle\\ &= |\langle 0|E^{(+)}(\mathbf{R},t)|\psi_F\rangle|^2,\end{aligned} \tag{36}$$

where $|\psi_F\rangle = \sum_{\mathbf{k}} C_{\mathbf{k}}(\infty)\,|1_{\mathbf{k}}\rangle$ is the final state. The value of $C_{\mathbf{k}}(\infty)$ can be obtained from Eq. (18), and we have

$$C_{\mathbf{k}}(\infty) = -i\sum_n V_{\mathbf{k},eg}e^{-i\mathbf{k}\cdot\mathbf{r}_n}\int_0^\infty e^{-i(\omega'_{eg}-\omega_k)t}C_n(t')dt'. \tag{37}$$

For an initial state $|\psi(0)\rangle = \sum_m a_m\,|\Gamma_m\rangle$, we already know its time evolution $|\psi(t)\rangle = \sum_m a_m e^{-\Gamma_m t}\,|\Gamma_m\rangle$ [Eq. (27)], and consequently, we have

$$\begin{aligned}C_n(t) &= \langle e_n|\,\psi(t)\rangle\\ &= \sum_m a_m e^{-\Gamma_m t}\,\langle e_n|\,\Gamma_m\rangle = \sum_m a_m b_n^{(m)} e^{-\Gamma_m t}.\end{aligned} \tag{38}$$

Here $b_n^{(m)} = \langle e_n|\,\Gamma_m\rangle$ is the projection of the eigenstate $|\Gamma_m\rangle$ on the single-atom excited state $|e_n;0\rangle$. Substituting Eq. (38) into Eq. (37), we get

$$\begin{aligned}C_{\mathbf{k}}(\infty) &= -i\sum_n V_{eg,\mathbf{k}}e^{-i\mathbf{k}\cdot\mathbf{r}_n}\int_0^\infty e^{-i(\omega'_{eg}-\omega_k)t}\\ &\quad\times\sum_m a_m b_n^{(m)}e^{-\Gamma_m t}dt'\\ &= -i\sum_n\sum_m V_{eg,\mathbf{k}}e^{-i\mathbf{k}\cdot\mathbf{r}_n}\frac{a_m b_n^{(m)}}{\Gamma_m - i(\omega_k-\omega'_{eg})}.\end{aligned} \tag{39}$$

Then we have

$$\begin{aligned}&\langle 0|\,E^{(+)}(\mathbf{R},t)\,|\psi_F\rangle\\ &= \langle 0|\sum_{\mathbf{k}}\sqrt{\frac{\omega_k}{2\varepsilon_0 V}}b_{\mathbf{k}}\hat{e}_{\mathbf{k}}e^{-i\omega_k t+i\mathbf{k}\cdot\mathbf{R}}\sum_{\mathbf{k}}C_{\mathbf{k}}(\infty)\,|1_{\mathbf{k}}\rangle\\ &= \frac{-iV}{(2\pi)^3}\int d\Omega\int k^2dk\sqrt{\frac{\omega_k}{2\varepsilon_0 V}}\hat{e}_{\mathbf{k}}e^{-i\omega_k t+i\mathbf{k}\cdot\mathbf{R}}\\ &\quad\times\sum_n\sum_m V_{\mathbf{k},eg}e^{-i\mathbf{k}\cdot\mathbf{r}_n}\frac{a_m b_n^{(m)}}{\Gamma_m - i(\omega_k-\omega'_{eg})}\\ &= \frac{-i}{2\varepsilon_0(2\pi)^3}e^{-i\omega_k t}\omega_{eg}\int k^2dk\int d\Omega\hat{e}_{\mathbf{k}}(\hat{e}_{\mathbf{k}}\cdot\hat{\mathbf{d}}_{eg})e^{i\mathbf{k}\cdot\mathbf{R}_n}\\ &\quad\times\frac{2\omega_{eg}}{\omega_{eg}+\omega_k}\sum_n\sum_m\frac{a_m b_n^{(m)}}{\Gamma_m - i(\omega_k-\omega'_{eg})},\end{aligned} \tag{40}$$

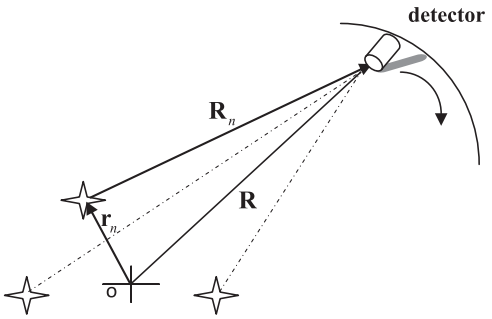

FIG. 7. The schematic description of the relation between the detector and the three atoms.

where $\mathbf{R}_n \equiv \mathbf{R} - \mathbf{r}_n$. The relations between the detector and the three atoms are schematically plotted in Fig. 7.

Note that the detector is far away from the atoms in experiment ($R \gg \lambda_0$). The optical mode whose wave vector is not parallel to $\hat{\mathbf{R}}_n$ leads to negligible contributions to the detector, so $\hat{\mathbf{k}}$ is replaced by $\hat{\mathbf{R}}_n$. Meanwhile, we use the approximation $R_n \approx R$ and $\hat{\mathbf{R}}_n \approx \hat{\mathbf{R}}$ except for the phases of the exponential function. The integral over the angle Ω of the electromagnetic modes can be written as

$$\begin{aligned}
&\int d\Omega \hat{e}_k (\hat{e}_{\mathbf{k}} \cdot \hat{\mathbf{d}}_{eg}) e^{i\mathbf{k}\cdot\mathbf{R}_n} \\
&= \int d\Omega [\hat{\mathbf{d}}_{eg} - \hat{\mathbf{k}}(\hat{\mathbf{k}} \cdot \hat{\mathbf{d}}_{eg})] e^{i\mathbf{k}\cdot\mathbf{R}_n} \\
&\approx [\hat{\mathbf{d}}_{eg} - \hat{\mathbf{R}}_n(\hat{\mathbf{R}}_n \cdot \hat{\mathbf{d}}_{eg})] \int_0^{2\pi} d\varphi \int_0^{\pi} e^{ikR_n \cos\theta} \sin\theta d\theta \\
&\approx [\hat{\mathbf{R}} \times (\hat{\mathbf{d}}_{eg} \times \hat{\mathbf{R}})] \frac{2\pi}{ikR} (e^{ikR_n} - e^{-ikR_n}). \qquad (41)
\end{aligned}$$

Substituting Eq. (41) into Eq. (40), and only retaining the outward wave with the phase factor $e^{i(kR_n - \omega t)}$ [28], we get

$$\begin{aligned}
&\langle 0|E^{(+)}(\mathbf{R},t) \sum_{\mathbf{k}} C_{\mathbf{k}}(\infty)|1_{\mathbf{k}}\rangle \\
&= \frac{-\omega_{eg}[\hat{\mathbf{R}} \times (\hat{\mathbf{d}}_{eg} \times \hat{\mathbf{R}})]}{i\varepsilon_0 (2\pi)^2 Rc^2} \int \omega_k d\omega_k \frac{\omega_{eg}}{\omega_{eg} + \omega_k} e^{-i\omega_k t} \\
&\quad \times \sum_n \sum_m \frac{e^{ikR_n} a_m b_n^{(m)}}{\Gamma_m - i(\omega_k - \omega'_{eg})} \\
&= \int d\omega_k e^{-i\omega_k t} B_{\mathbf{R}}(\omega_k), \qquad (42)
\end{aligned}$$

where

$$\begin{aligned}
B_{\mathbf{R}}(\omega_k) = &\frac{\hat{\mathbf{R}} \times (\hat{\mathbf{d}}_{eg} \times \hat{\mathbf{R}})}{4i\varepsilon_0 \pi^2 Rc^2} \frac{\omega_{eg}^2 \omega_k}{\omega_{eg} + \omega_k} \\
&\times \sum_n \sum_m \frac{e^{ikR_n} a_m b_n^{(m)}}{\Gamma_m - i(\omega_k - \omega'_{eg})}. \qquad (43)
\end{aligned}$$

The spectrum detected by the detector at $\mathbf{R}$ is given by [23]

$$\begin{aligned}
S_R(\omega_k) &\propto |B_R(\omega_k)|^2 \\
&\propto \left| \hat{\mathbf{R}} \times (\hat{\mathbf{d}}_{eg} \times \hat{\mathbf{R}}) \sum_n \sum_m \frac{e^{ikR_n} a_m b_n^{(m)}}{\Gamma_m - i(\omega_k - \omega'_{eg})} \right|^2, \qquad (44)
\end{aligned}$$

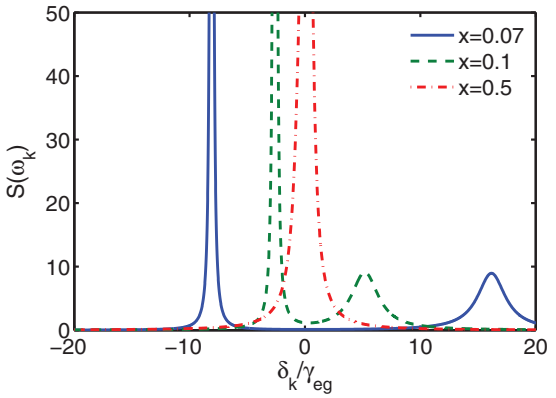

FIG. 8. (Color online) The total spectrum (in arbitrary units) for the equilateral-triangle configuration with the initial state of which only the first atom is excited. x is the side length of the triangle and $\eta_{mn} = \pi/2$.

which is the spectrum in a particular direction. Sometimes the total spectrum integrated over all detector directions is more important, which is the average of the spectra detected by all detectors in each direction [23].

Integrating the spectrum over all the detector directions, one obtains the total spectrum

$$S(\omega_k) = \int d\Omega_{\boldsymbol{R}} S_{\boldsymbol{R}}(\omega_k) = \sum_{n,n'} f_n(k) f_{n'}^*(k) T_{nn'}(k), \qquad (45)$$

where

$$f_n(k) = \sum_m \frac{a_m b_n^{(m)}}{\Gamma_m - i(\omega_k - \omega'_{eg})}, \qquad (46)$$

$$\begin{aligned}
T_{nn'}(k) &= \int d\Omega_R [\hat{\mathbf{R}} \times (\hat{\mathbf{d}}_{eg} \times \hat{\mathbf{R}})]^2 e^{ikr_{nn'}} \\
&= \begin{cases} 8\pi/3 & (n' = n) \\ 4\pi D(x_{nn'}, \eta_{nn'}) & (n' \neq n) \end{cases}. \qquad (47)
\end{aligned}$$

$\eta_{nn'}$ is the angle between $\mathbf{r}_{nn'}$ and $\hat{\mathbf{d}}_{eg}$, and $D(x_{nn'}, \eta_{nn'})$ is the function defined in Eq. (23).

As the spectrum depends on the initial state of the system, we first assume the first atom initially in the excited state and the other two in the ground states, $|\psi_0\rangle = |e_1; 0\rangle$. By using Eq. (45), we can plot the total spectrum of the three-atom system. First, we study the spectrum for the atomic configuration of the equilateral triangle. We define the detuning as $\delta_k \equiv \omega_k - \omega_{eg}^s$, where $\omega_{eg}^s = \omega'_{eg} + \Delta_{eg}$ is the single atomic transition frequency including the Lamb shift [23]. From Eqs. (32) and (46), we know that the spectrum will have two peaks at $\delta_k = \gamma_{eg} P(x, \frac{\pi}{2})$ and $\delta_k = -\frac{\gamma_{eg}}{2} P(x, \frac{\pi}{2})$. In Fig. 8, we plot the total spectra of this special case, where we can see that when the atoms are placed very near to each other, the interaction between the atoms splits the spectrum into two peaks (see the blue solid and green dash curves in Fig. 8, for $x = 0.07$, 0.1 respectively); the wide one (corresponding to super-radiance) relates to the eigenstate $|a\rangle$ and the narrow one (subradiance) relates to the degenerate eigenstates $|b\rangle$ and $|c\rangle$. As the distance increases, the two peaks merge into one peak (see red dash dot curve), and finally the spectrum tends to be the single-atom Lorentzian peak. If the three-atom system

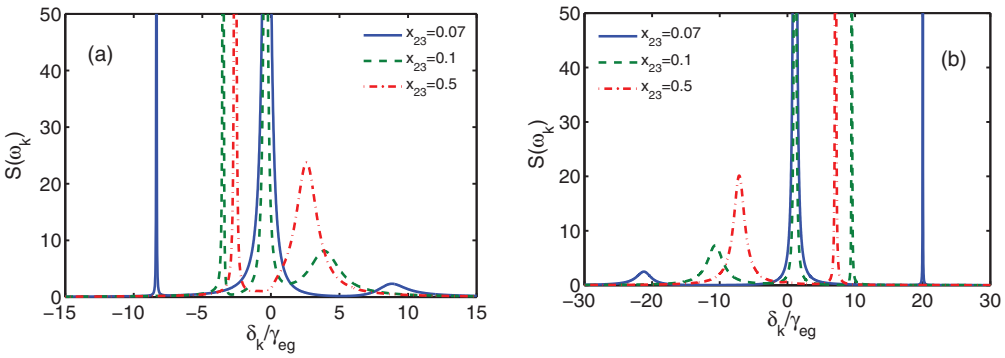

FIG. 9. (Color online) The total spectrum (in arbitrary units) for the case where three atoms are arranged in a straight line with different direction of dipole moment (a) $\eta_{mn} = \pi/2$ and (b) $\eta_{mn} = 0$. Here $x_{12} = 0.1$.

is initially prepared in the Dicke state, that is, the eigenstate $|a\rangle$ in this case, the spectrum will have only one peak.

Next, we study the spectra for general atomic configuration. As mentioned above, the general-triangle configuration is similar to the straight-line configuration, so we just discuss the spectra for the latter one. Like the study of decay rate, we focus on the strong coupling system, so we select a small distance between the left two atoms $x_{12} = 0.1$ (please refer to Fig. 2), then change the position of the third one. Here, we still choose $|\psi_0\rangle = |e_1; 0\rangle$ as the initial state of the system. In Fig. 9, we plot the total spectra for this case with three different values of x_{23}. Meanwhile we also want to see the influence of the direction of dipole moment on the collective Lamb shift, so we select $\eta_{mn} = \frac{\pi}{2}$ and $\eta_{mn} = 0$; see Figs. 9(a) and 9(b), respectively.

When the three atoms are placed in a short distance, the emission spectra have three peaks; see the blue solid and green dash curves in Fig. 9. The wide peak corresponds to the super-radiant state, and the other two narrow ones come from two subradiant states. With the third atom being put far away from the left two atoms along the line, the coherence between it and the other two atoms weakens, so the collective Lamb shift is receded. When the third atom is far enough away from the other two, the three-atom system reduces to the two-atom system which has a two-peak spectrum (see the red dash dot curve). Note that the collective Lamb shift always increases with decreasing the distance x_{23}, and it is mainly dependent on the shortest distance of the three atomic distances. This is different from the decay rate [see Fig. 4(c)], and there is no symmetric effect for the collective Lamb shift.

In Fig. 9(a), when $\eta = \frac{\pi}{2}$, the super-radiant state (corresponding to the widest peak) is blueshifted while in Fig. 9(b), when $\eta = 0$, the super-radiant state is redshifted. This η dependence of the shift can be explained with the function $P(x,\eta)$ in Fig. 2(b). In a short distance, $P(x,\eta = \frac{\pi}{2})$ stands for a repulsive interaction, while $P(x,\eta = 0)$ stands for an attractive interaction. As a result, the super-radiant state will have higher energy (blueshift) when $\eta = \frac{\pi}{2}$, and lower energy (redshift) when $\eta = 0$.

VI. SUMMARY

In this paper, we investigate the cooperative spontaneous emission of the system consisting of three identical multi-level atoms in vacuum field by the optical vector method. The problem of dynamic evolution is transformed to the eigenvalue problem of a 3×3 matrix, and we obtain the analytic expression of the three eigenvalues and apply it to the equilateral-triangle, straight-line, and general-triangle atomic configurations. The Dicke state for a three-atom system (i.e., the W entangled state) is an exponentially decaying eigenstate only for the equilateral-triangle configuration. For a multiatom system ($N > 3$), the Dicke state could not exactly be an exponentially decaying eigenstate, no matter what the configuration is. The atomic configuration (distribution) has great influence on the super-radiance. To obtain strong super-radiance requires not only the distances among the three atoms to be much shorter than the wavelength, but to also have symmetrical distribution. However, the symmetry has little effect on the collective Lamb shift. Large collective Lamb shift mainly depends on the shortest distance of three atomic distances. The emission spectrum normally has three peaks and the spectral structure also depends on the direction of the dipole moment. For the equilateral-triangle configuration, there are only two peaks due to the symmetry of the configuration.

ACKNOWLEDGMENTS

We thank Jörg Evers and Jin-Ze Wu for helpful discussions. This work was supported by the National Natural Science Foundation of China (under Grants No. 11174026 and No. 11174027) and the National Basic Research Program of China (Grants No. 2011CB922203 and No. 2012CB922104).

APPENDIX: CALCULATION OF THE MATRIX ELEMENTS IN EQ. (20)

We rewrite Eq. (20) here,

$$\dot{C}_n(t) \approx -C_n(t)\sum_{\mathbf{k}} V_{\mathbf{k},eg}^2 \int_{-\infty}^{t} e^{i(\omega'_{eg}-\omega_k)(t-t')}dt' - C_m(t)\sum_{m\neq n}\left[\sum_{\mathbf{k}} V_{\mathbf{k},eg}^2 e^{ikr_{nm}} \int_{-\infty}^{t} e^{i(\omega'_{eg}-\omega_k)(t-t')}dt' + i\Delta_{sta}^{mn}\right] = -\Gamma_0 C_n(t) - \sum_{m\neq n}\Gamma_{mn}C_m(t), \quad \text{(A1)}$$

where

$$\Gamma_0 = \sum_{\mathbf{k}} V_{\mathbf{k},eg}^2 \left[\pi\delta(\omega'_{eg} - \omega_k) + i\mathrm{P}\frac{1}{\omega'_{eg} - \omega_k} \right], \tag{A2}$$

$$\Gamma_{mn} = \sum_{\mathbf{k}} V_{\mathbf{k},eg}^2 e^{i\mathbf{k}\cdot\mathbf{r}_{nm}} [\pi\delta(\omega'_{eg} - \omega_k)] + i\left(\Delta_{sta}^{mn} + \mathrm{P}\sum_{\mathbf{k}} V_{\mathbf{k},eg}^2 e^{i\mathbf{k}\cdot\mathbf{r}_{nm}} \frac{1}{\omega'_{eg} - \omega_k} \right). \tag{A3}$$

In the above equation, we have used the integral formula $\int_{-\infty}^{t} dt' e^{ix(t-t')} = \pi\delta(x) + i\mathrm{P}\frac{1}{x}$, where P stands for principal part. Detailed calculation gives

$$\begin{aligned}
\Gamma_0 &= \sum_{\mathbf{k}} V_{\mathbf{k},eg}^2 \left[\pi\delta(\omega'_{eg} - \omega_k) + i\mathrm{P}\frac{1}{\omega'_{eg} - \omega_k} \right] = \frac{d_{eg}^2\omega_{eg}^2}{6\pi^2\varepsilon_0 c^3} \int_0^\infty \omega_k \frac{4\omega_{eg}^2}{(\omega_k + \omega_{eg})^2} \left[\pi\delta(\omega'_{eg} - \omega_k) + i\mathrm{P}\frac{1}{\omega'_{eg} - \omega_k} \right] d\omega_k \\
&\approx \frac{d_{eg}^2\omega_{eg}^2}{6\pi^2\varepsilon_0 c^3} \int_0^\infty \omega_k \frac{4\omega_{eg}^2}{(\omega_k + \omega_{eg})^2} \left[\pi\delta(\omega_{eg} - \omega_k) + i\mathrm{P}\frac{1}{\omega_{eg} - \omega_k} \right] d\omega_k \\
&= \frac{1}{2}\frac{d_{eg}^2\omega_{eg}^3}{3\pi\varepsilon_0 c^3} + i\frac{d_{eg}^2\omega_{eg}^2}{6\pi^2\varepsilon_0 c^3}\mathrm{P}\int_0^\infty \frac{\omega_k}{\omega_{eg} - \omega_k}\frac{4\omega_{eg}^2}{(\omega_k + \omega_{eg})^2} d\omega_k = \frac{\gamma_{eg}}{2} + i\Delta_{eg},
\end{aligned} \tag{A4}$$

where

$$\Delta_{eg} = \frac{d_{eg}^2\omega_{eg}^2}{6\pi^2\varepsilon_0 c^3}\mathrm{P}\int_0^\infty \frac{\omega_k}{\omega_{eg} - \omega_k}\frac{4\omega_{eg}^2}{(\omega_k + \omega_{eg})^2} d\omega_k \tag{A5}$$

is the dynamic shift of single atoms. Note that we approximate $\omega'_{eg} \approx \omega_{eg}$ and ignore the nondynamic shift for single atoms in Eq. (A5), because this part is negligible compared with the dynamic shift [21]. The real part of Γ_{mn} is

$$\begin{aligned}
\mathrm{Re}\,(\Gamma_{mn}) &= \sum_{\mathbf{k}} V_{\mathbf{k},eg}^2 e^{i\mathbf{k}\cdot\mathbf{r}_{mn}} [\pi\delta(\omega_{eg} - \omega_k)] \\
&= \frac{d_{eg}^2\omega_{eg}^2}{6\pi\varepsilon_0 c^3} \int_0^\infty \left[\frac{2\omega_{\mathrm{eg}}}{(\omega_{\mathrm{eg}} + \omega_k)} \right]^2 \omega_k D\,(kr_{mn}/2\pi, \eta_{mn})\,\delta(\omega_{eg} - \omega_k) d\omega_k, \\
&= \frac{\gamma_{eg}}{2} D\,(x_{mn}, \eta_{mn})\,,
\end{aligned} \tag{A6}$$

where we change the summation over $\mathbf{k}$ to an integration (see Ref. [6], p.7),

$$\sum_{\mathbf{k}} g_{\mathbf{k},eg}^2 e^{i\mathbf{k}\cdot\mathbf{r}_{mn}} \to \frac{d_{eg}^2\omega_{eg}^2}{6\pi^2\varepsilon_0 c^3} \int_0^\infty \omega_k D\,(kr_{mn}/2\pi, \eta_{mn})\, d\omega_k. \tag{A7}$$

$D\,(x_{mn}, \eta_{mn})$ is defined in Eq. (23). The imaginary part of Γ_{mn} is

$$\begin{aligned}
\mathrm{Im}\,(\Gamma_{mn}) &= \left(\Delta_{sta}^{mn} + \mathrm{P}\sum_{\mathbf{k}} V_{\mathbf{k},eg}^2 e^{i\mathbf{k}\cdot\mathbf{r}_{mn}} \frac{1}{\omega'_{eg} - \omega_k} \right) \\
&= \frac{1}{4\pi\varepsilon_0}\left[\frac{\mathbf{d}_{eg}^{(m)}\cdot\mathbf{d}_{ge}^{(n)}}{r_{mn}^3} - \frac{3\left(\mathbf{d}_{eg}^{(m)}\cdot\mathbf{r}_{mn}\right)\left(\mathbf{d}_{ge}^{(n)}\cdot\mathbf{r}_{mn}\right)}{r_{mn}^5} \right] - \sum_{\mathbf{k}} \frac{2g_{\mathbf{k},\mathrm{eg}}^2\xi_{k,eg}}{\omega_k}(2 - \xi_{k,eg}) e^{i\mathbf{k}\cdot\mathbf{r}_{mn}} + \mathrm{P}\sum_{\mathbf{k}} V_{\mathbf{k},eg}^2 e^{i\mathbf{k}\cdot\mathbf{r}_{mn}} \frac{1}{\omega'_{eg} - \omega_k} \\
&= \frac{1}{4\pi\varepsilon_0}\left[\frac{\mathbf{d}_{eg}^{(m)}\cdot\mathbf{d}_{ge}^{(n)}}{r_{mn}^3} - \frac{3\left(\mathbf{d}_{eg}^{(m)}\cdot\mathbf{r}_{mn}\right)\left(\mathbf{d}_{ge}^{(n)}\cdot\mathbf{r}_{mn}\right)}{r_{mn}^5} \right] - \frac{d_{eg}^2\omega_{eg}^2}{6\pi^2\varepsilon_0 c^3}\int_0^\infty \frac{2(\omega_k + 2\omega_{\mathrm{eg}})\omega_k}{(\omega_{\mathrm{eg}} + \omega_k)^2} D(kr_{mn}/2\pi, \eta_{mn}) d\omega_k \\
&\quad + \frac{d_{eg}^2\omega_{eg}^2}{6\pi^2\varepsilon_0 c^3}\mathrm{P}\int_0^\infty \frac{\omega_k}{(\omega_{\mathrm{eg}} - \omega_k)}\frac{4\omega_{eg}^2}{(\omega_{\mathrm{eg}} + \omega_k)^2} D(kr_{mn}/2\pi, \eta_{mn}) d\omega_k \\
&= \frac{1}{4\pi\varepsilon_0}\left[\frac{\mathbf{d}_{eg}^{(m)}\cdot\mathbf{d}_{ge}^{(n)}}{r_{mn}^3} - \frac{3(\mathbf{d}_{eg}^{(m)}\cdot\mathbf{r}_{mn})(\mathbf{d}_{ge}^{(n)}\cdot\mathbf{r}_{mn})}{r_{mn}^5} \right] + \frac{d_{eg}^2\omega_{eg}^2}{6\pi^2\varepsilon_0 c^3}\mathrm{P}\int_{-\infty}^\infty \frac{\omega_k^2}{\omega_{eg}^2 - \omega_k^2} D\,(kr_{mn}/2\pi, \eta_{mn})\, d\omega_k \\
&= \frac{d_{eg}^2}{4\pi\varepsilon_0 r_{mn}^3}(1 - 3\cos^2\eta_{mn}) + \frac{\gamma_{eg}}{2}\frac{3}{2}\left\{ -\sin^2\eta_{mn}\frac{\cos(2\pi x_{mn})}{2\pi x} + (1 - 3\cos^2\eta)\left[\frac{\sin(2\pi x_{mn})}{(2\pi x_{mn})^2} + \frac{\cos(2\pi x_{mn}) - 1}{(2\pi x_{mn})^3} \right] \right\} \\
&= \frac{\gamma_{eg}}{2} P(x_{mn}, \eta_{mn}),
\end{aligned} \tag{A8}$$

where the principal value integral $\mathrm{P}\int_{-\infty}^{\infty}\frac{\omega_k^2}{\omega_{eg}^2 - \omega_k^2} D\,(kr_{mn}/2\pi, \eta_{mn})\, d\omega_k\, D\,(x_{mn}, \eta_{mn})$ has three poles on the x axis, $\pm\omega_{eg}$ and 0, which can be shown by contour integration. $P(x_{mn}, \eta_{mn})$ is defined in Eq. (24).

[1] R. H. Dicke, Phys. Rev. **93**, 99 (1954).
[2] J. W. Czarnik and P. R. Fontana, J. Chem. Phys. **50**, 4071 (1969).
[3] R. H. Lehmberg, Phys. Rev. A **2**, 883 (1970); **2**, 889 (1970).
[4] N. E. Rehler and J. H. Eberly, Phys. Rev. A **3**, 1735 (1971).
[5] J. C. MacGillivray and M. S. Feld, Phys. Rev. A **14**, 1169 (1976).
[6] G. S. Agarwal, in *Quantum Statistical Theories of Spontaneous Emission and Their Relation to Other Approaches*, edited by G. Höhler, Springer Tracts in Modern Physics Vol. 70 (Springer-Verlag, Berlin, 1974).
[7] M. Kiffner, M. Macovei, J. Evers, and C. H. Keitel, in *Vacuum-Induced Processes in Multi-Level Atoms*, edited by E. Wolf, Progress in Optics Vol. 55 (Elsevier, Amsterdam, 2010).
[8] M. O. Scully, Phys. Rev. Lett. **102**, 143601 (2009).
[9] A. A. Svidzinsky and J.-T. Chang, Phys. Lett. A **372**, 5732 (2008).
[10] A. A. Svidzinsky and M. O. Scully, Opt. Commun. **282**, 2894 (2009).
[11] A. A. Svidzinsky, J.-T. Chang, and M. O. Scully, Phys. Rev. A **81**, 053821 (2010).
[12] M. O. Scully and A. A. Svidzinsky, Science **325**, 1510 (2009); **328**, 1239 (2010).
[13] R. Friedberg and J. T. Manassah, Phys. Lett. A **372**, 2514 (2008).
[14] R. Friedberg and J. T. Manassah, Opt. Commun. **281**, 4391 (2008).
[15] R. Friedberg and J. T. Manassah, Phys. Rev. A **81**, 043845 (2010).
[16] R. Röhlsberger, K. Schlage, B. Sahoo, S. Couet, and R. Rüffer, Science **328**, 1248 (2010).
[17] J. Keaveney, A. Sargsyan, U. Krohn, I. G. Hughes, D. Sarkisyan, and C. S. Adams, Phys. Rev. Lett. **108**, 173601 (2012).
[18] Y. Li, J. Evers, H. Zheng, and S.-Y. Zhu, Phys. Rev. A **85**, 053830 (2012).
[19] Y. Li, J. Evers, W. Feng, and S.-Y. Zhu, Phys. Rev. A **87**, 053837 (2013).
[20] H. Zheng, S.-Y. Zhu, and M. S. Zubairy, Phys. Rev. Lett. **101**, 200404 (2008).
[21] Z.-H. Li, D.-W. Wang, H. Zheng, S.-Y. Zhu, and M. S. Zubairy, Phys. Rev. A **80**, 023801 (2009).
[22] D. W. Wang, A.-J. Li, L.-G. Wang, S.-Y. Zhu, and M. S. Zubairy, Phys. Rev. A **80**, 063826 (2009).
[23] D. W. Wang, Z. H. Li, H. Zheng and S.-Y. Zhu, Phys. Rev. A **81**, 043819 (2010).
[24] T. Brandes and B. Kramer, Phys. Rev. Lett. **83**, 3021 (1999).
[25] M. Scheibner, T. Schmidt, L. Worschech, A. Forchel, G. Bacher, T. Passow, and D. Hommel, Nat. Phys. **3**, 106 (2007).
[26] S. Mokhlespour, J. E. M. Haverkort, G. Slepyan, S. Maksimenko, and A. Hoffmann, Phys. Rev. B **86**, 245322 (2012).
[27] M. Kozub, Ł. Pawicki, and P. Machnikowski, Phys. Rev. B **86**, 121305 (2012).
[28] M. O. Scully and M. S. Zubairy, *Quantum Optics* (Cambridge University Press, Cambridge, 1997).